The Preparation and Characterization of Carboxylic Acid-Coated Silica Nanoparticles

Brandon M. Cash, Lei Wang, Brian C. Benicewicz

Department of Chemistry and Biochemistry and USC NanoCenter, University of South Carolina, Columbia, South Carolina 29208
Correspondence to: B. C. Benicewicz (E-mail: benice@sc.edu)

Received 15 November 2011; accepted 19 February 2012; published online 27 March 2012
DOI: 10.1002/pola.26029

ABSTRACT: The preparation of carboxylic acid-coated silica nanoparticles was investigated. A monolayer of carboxylic acid residues with controllable graft density was anchored to the nanoparticle by a ring-opening reaction with succinic anhydride. Poly(methacrylic acid) [poly(MAA)] grafted nanoparticles were prepared via a polymerization–deprotection strategy. *Tert*-butyl methacrylate was polymerized from the surface of silica nanoparticles in a predictable manner and with excellent control over the molecular weight distribution. Subsequent removal of the *tert*-butyl group resulted in poly (MAA) grafted nanoparticles. The polymer nanoparticles were also functionalized with dyes, which may be useful in tracking the particles in biological systems. © 2012 Wiley Periodicals, Inc. J Polym Sci Part A: Polym Chem 50: 2533–2540, 2012

KEYWORDS: living polymerization; nanocomposites; nanoparticles; reversible addition fragmentation chain transfer (RAFT)

INTRODUCTION Reversible addition-fragmentation chain transfer (RAFT) has emerged as a powerful reversible addition radical polymerization technique to prepare polymeric materials with predictable molecular weights and narrow polydispersities. Moad and coworkers[1] founded RAFT polymerizations that are conducted under mild conditions, free of metal catalysts, and compatible with nearly all monomers that can be polymerized via conventional free radical polymerization techniques. The mechanism of RAFT polymerization is based on a sequence of chain transfer reactions. At the outset of a typical RAFT polymerization, a radical initiator is decomposed and forms a short propagating radical ($P_{n\bullet}$), which subsequently adds to a chain transfer agent. This is followed by a fragmentation step releasing the radical $R^{\bullet}$. The newly formed radical reinitiates the polymerization by adding to additional monomer in solution to form a new propagating radical ($P_{m\bullet}$). Following the creation of ($P_{m\bullet}$), a rapid equilibrium is established between propagating radicals, ($P_{m\bullet}$) and ($P_{n\bullet}$), and the dormant polymeric thiocarbonylthio end-capped chains. A fast equilibrium must be established for all chains to grow in an equal manner, thus establishing polymers with narrow polydispersties.[1–5]

The preparation of polymer nanocomposites by the surface modification of nanoparticles has drawn considerable interest due to their potential applications in optics, electronics, and bioapplications.[6–9] The RAFT technique has proven to be a versatile method for the modification of surfaces with polymeric materials due to the ease in which RAFT agents can be attached to surfaces and the excellent control over surface graft density. Fukuda and coworkers[10] reported the first application of RAFT-mediated polymerization of styrene from the surface of silica particles utilizing a surface-anchored RAFT agent. Following this pioneering work, surface-initiated RAFT polymerization has been widely used to modify a variety of surfaces with different polymers.[11–13]

Polymers bearing numerous environmentally/stimuli-responsive functionalities represent an important category of macromolecules due to potential uses such as their ability to mimic biological surfaces, drug-delivery agents, controlled-release coatings, biomolecule immobilization, sensing applications, and membrane transport.[14] In particular, materials bearing poly(acrylic acid) (PAA) or poly(methacrylic acid) [poly(MAA)] residues have become increasingly important due to their aqueous solubility, polyelectrolyte character, and their ability to conjugate biologically active molecules. Despite the many current and emerging applications, there have been relatively few reports regarding the synthesis of carboxylic acid bearing nanoparticles and/or surfaces in a direct albeit controllable manner. For instance, utilizing surface-initiated atom transfer radical polymerization (SI-ATRP), Brittain and coworkers[13] prepared poly(*tert*-butylacrylate) brushes from the surface of silica. Subsequent heating of the samples to 200 °C induced pyrolysis leading to PAA grafted wafers. In a different report yet similar approach, Genzer[15] and coworkers reported the fabrication of PAA grafted materials by polymerizing *tert*-butylacrylate from the surface of

silicon wafers utilizing SI-ATRP followed by dilute acid hydrolysis of the *tert*-butyl ester. In an effort to engineer environmentally responsive nanoparticles, Zhao and coworkers synthesized mixed homopolymer brushes via a sequential ATRP polymerization of *tert*-butylacrylate and nitroxide-mediated radical polymerization of styrene from the surface of a nanoparticle modified with a Y-initiator. Removal of the *tert*-butyl groups using iodotrimethylsilane (TMSI) resulted in environmentally responsive amphiphilic silica nanoparticles.[16] In a direct approach for the fabrication of PAA grafted from the surface of nanoparticles, Charpentier and coworkers[17] functionalized TiO_2 nanoparticles with a carboxylic acid-functionalized RAFT agent followed by polymerization with acrylic acid. Inoue et al.[18] prepared poly(6-(acrylamide)hexanoic acid grafted silica nanoparticles that flocculated at lower pHs because of the hydrophobic interactions of the pendant chains but could be dispersed at higher pHs because of the electrostatic repulsion of the carboxylate ions.

Resistant microbial infections in the form of bacterial biofilms have become wide spread with an ever-increasing mortality rate.[19] Biofilm infections are significantly more difficult to treat using traditional therapies due to a protective barrier that defends the bacterial cells from antibiotics. Furthermore, biofilm infections have the ability to coordinate their metabolic activity using a communication method called quorum sensing. This method of communication allows the bacterial cells to operate, communicate, and function as a group rather than single bacterial cells. Most importantly, antibiotic resistance genes can be rapidly transferred to other cells leading to an overall enhanced antibiotic resistance.[20–23]

Although antibiotics bound to nanoparticles have been utilized to efficiently kill bacteria in liquid cultures, this type of drug-delivery method has not been extensively investigated for the treatment of biofilm-mediated microbial infections.[24,25] Preliminary investigations have shown that a low density of antibiotics nonspecifically bound to nanoparticles via sulfate or carboxyl groups is more efficient at killing bacteria than antibiotics administered in solution. In addition to the increased efficacy of the bound antibiotics, nanoparticles coated with carboxyl groups readily penetrated biofilms up to 50 μm over a 24-h period. Based on these observations, engineering a nanoparticle with a controllable density of carboxyl groups capable of binding nonspecifically to antibiotics would enhance the ability to study and combat biofilm-related infections. Herein, we describe our efforts in preparing functional silica nanoparticles bearing various densities of carboxylic acid residues to expand the scope of engineering surface-modified nanoparticles for such applications via surface-initiated RAFT polymerizations, and postmodifications of these polymers.

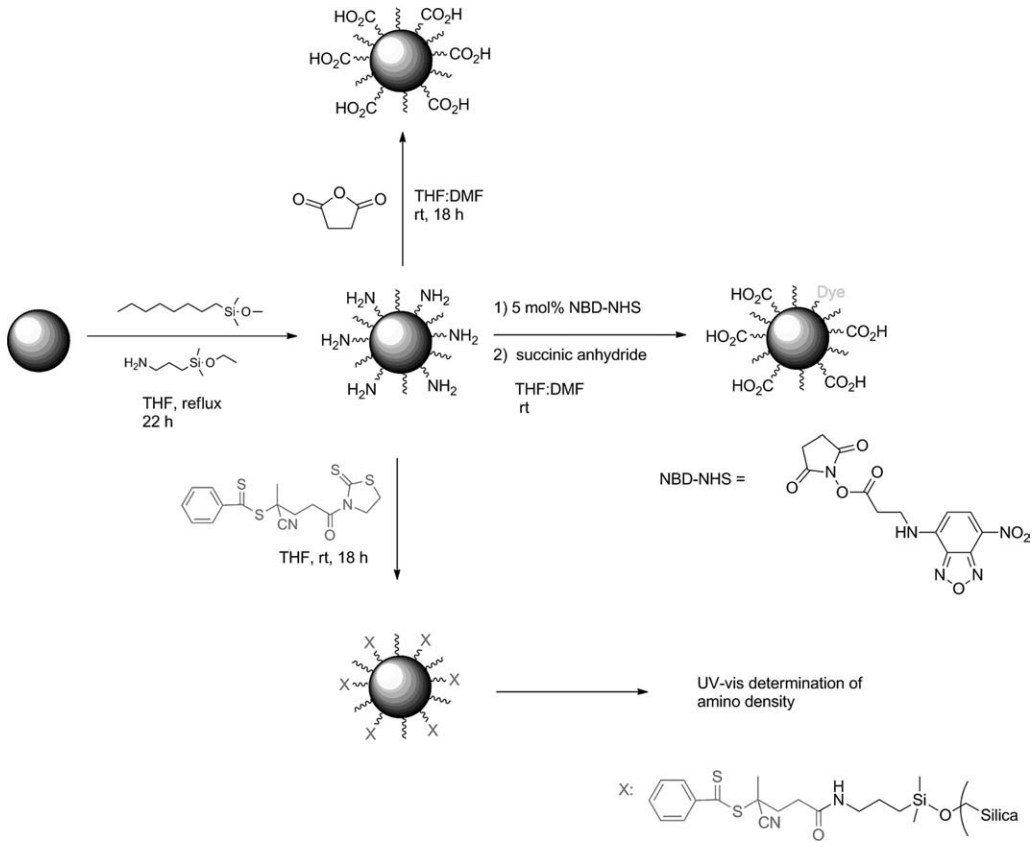

SCHEME 1 Preparation of carboxylic-coated silica nanoparticles.

RESULTS AND DISCUSSION

Silica nanoparticle surfaces bearing a thin monolayer of carboxylic acid residues were fabricated via a two-step procedure. Various densities of amine-functionalized nanoparticles ranging from 183 to 27 μmol/g were prepared according to the literature.[26] Briefly, commercially available silica nanoparticles (16–20 nm diameter, 30% in MEK) were treated with various feed ratios of octyl silane and amino silanes. The amine graft density was calculated by treating an aliquot of the amino-modified particles with excess activated 4-cyanopentanoic acid dithiobenzoate (CPDB) to ensure complete conversion of the amines followed by subsequent UV–vis analysis (Scheme 1).

Using a modified but similar procedure developed by Liu and coworkers, carboxyl groups were quantitatively introduced onto the nanoparticles by a ring-opening reaction of the amine-modified particles with succinic anhydride. The ring-opening reaction was monitored by the addition of salicylaldehyde to an aliquot of the reaction in progress. Unreacted amine-functionalized particles gave an immediate yellow color, whereas completely reacted particles remained colorless following treatment with salicylaldehyde.[27]

The resulting carboxylic acid-coated nanoparticles contain a large number of carboxy residues (100–1000—COOH/particle) and demonstrated increased solubility in alcoholic and/or aqueous media. Thermogravimetric analysis (TGA) of the modified particles confirmed the addition of organic groups after each reaction and was consistent with the UV analysis [Fig. 1(a)]. The FTIR spectrum of the carboxylic acid modified versus bare silica nanoparticles further demonstrated the modifications to the nanoparticles. As illustrated in Figure 1(b), characteristic absorption bands ascribed to the added carbonyl groups were evident at 1721.9 cm^{-1} and agrees with previous results from the literature.[28]

Using nanoparticles with precisely determined amine graft densities, bifunctional particles were easily prepared and further demonstrated the utility of the amine-functionalized particles. Dye-labeled carboxylic-coated nanoparticles were prepared by initially allowing the amine-coated particles to react with a submolar amount, 5 mol % relative to the amines, of activated nitrobenzofurazan derivative followed by an excess of succinic anhydride.[29] This protocol yields bifunctional particles labeled with a smaller percentage of fluorescent tags relative to carboxylic acid groups (Scheme 1). The amount of dye covalently bound to the nanoparticle surface was determined quantitatively by comparing the absorbance at 326 nm for the dye-modified particles to a standard UV–vis absorption curve prepared from known amounts of free dye. The dye-labeled carboxylic acid-coated nanoparticle solution (in ethanol) is yellow and transparent (Fig. 2). These labeled particles may be useful for monitoring the presence and movement of particles, particularly for biological applications.

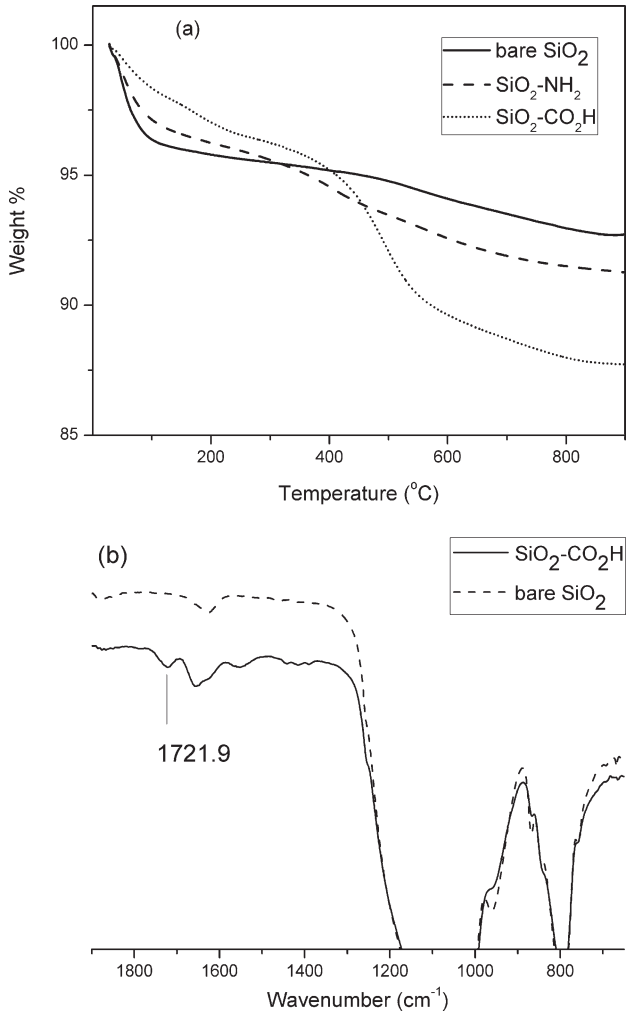

FIGURE 1 TGAs of bare SiO_2 nanoparticles (solid line), amino-coated SiO_2 nanoparticles (dashed line), and carboxylic acid SiO_2-coated nanoparticles (dotted line); (b) FTIR (thin film) of bare SiO_2 nanoparticles (dashed line) and carboxylic acid-coated nanoparticles (solid line).

Surface-Initiated RAFT Polymerization

The direct polymerization of MAA has been reported previously by a few groups in both organic solvents and water or mixed organic/aqueous solvents.[30–34] In this work, we chose to develop an organic solvent-based approach using a blocked MAA monomer, *tert*-butyl methacrylate (*t*BuMA), to utilize standard organic solvent-based GPC methods for molecular weight measurement, and to avoid either high or low pH environments in aqueous polymerization media, which might result in cleavage of the chains from the nanoparticle surface.

CPDB-anchored silica nanoparticles were prepared according to previous literature protocols and had a surface density of 22.04 μmol/g, which is equivalent to 0.093 chains/nm^2.[28] The surface-initiated RAFT polymerization of *t*BuMA was conducted at 60 °C utilizing AIBN as the radical initiator. A high ratio of surface-anchored CPDB to AIBN (10:1) was used to minimize free polymer from forming in solution. The surface graft polymerizations of *t*BuMA were conducted under dilute conditions in tetrahydrofuran (THF) containing a small percentage of anisole to easily monitor monomer

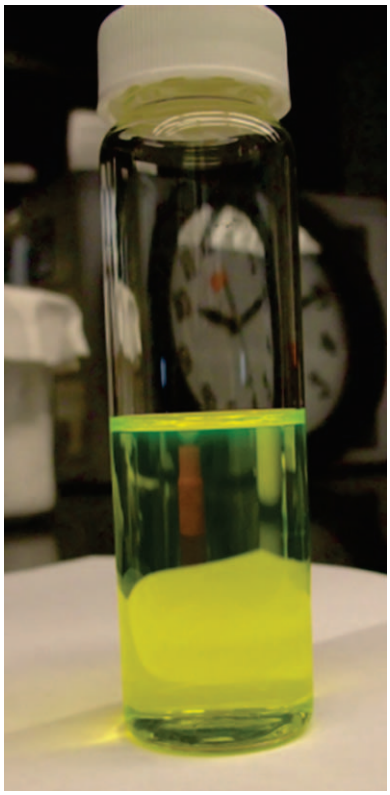

FIGURE 2 Photograph of dye-labeled carboxylic acid-coated nanoparticles in ethanol after several washes.

conversion by proton NMR. Typically, the polymerizations were carried out at a concentration of 2.4 mM with respect to the RAFT group and with a solvent to monomer ratio of 4:1. It is worth noting that more concentrated polymerizations yielded highly viscous reactions within a few hours and resulted in surface grafted polymers with increased molecular weight and polydispersity index (PDI). This could be a result of the Trommsdorff–Norrish effect, or autoacceleration effect, which predicts higher rates of polymerization with increased viscosity at the later stages of a polymerization.[35] The kinetic results of *t*BuMA polymerization mediated by CPDB-anchored nanoparticles are illustrated in Figure 3. A linear relationship between $\ln(M_0/M_t)$ (where M_0 is the initial monomer concentration and M_t is the monomer concentration at time t), and polymerization time was observed indicating a constant radical concentration throughout the polymerization. The controlled nature of the polymerization is demonstrated by the linear increase of M_n with respect to monomer conversion. In addition, excellent control over the PDI was observed over a range of monomer conversions. To investigate the effect of surface density of CPDB-anchored nanoparticles, polymerization of *t*BuMA mediated by CPDB-anchored nanoparticles with a higher surface density of 154.14 μmol/g, which is equivalent to 0.65 chains/nm^2, was conducted using similar conditions. The kinetic results are illustrated in Figure 4. A linear relationship between $\ln(M_0/M_t)$ and polymerization time was observed, and the molecular weight obtained from GPC was in excellent agreement with the theoretical molecular weight. The GPC traces for the surface-initiated RAFT polymerization of *t*BuMA from the silica nanoparticle (surface density: 22.04 μmol/g) are given in Figure 5. The traces were found to be monomodal and narrow over the conversion range investigated within this study.

Poly(MAA) Formation

The resulting surface grafted polymer chains contain *tert*-butyl ester side groups that can be deprotected to yield poly(MAA) grafted nanoparticles. Conventionally, *tert*-butyl protecting groups can be removed via acid hydrolysis, pyrolysis, or the use of TMSI.[13,15,16] Exposure of the *tert*-butyl grafted nanoparticles to acidic media such as trifluoroacetic acid and dilute aqueous acid, at various temperatures resulted in decomposition of the grafted nanoparticles. Furthermore, heating the surface grafted particles to temperatures of 150–200 °C to induce pyrolysis also led to decomposition of the RAFT agent end group and products that

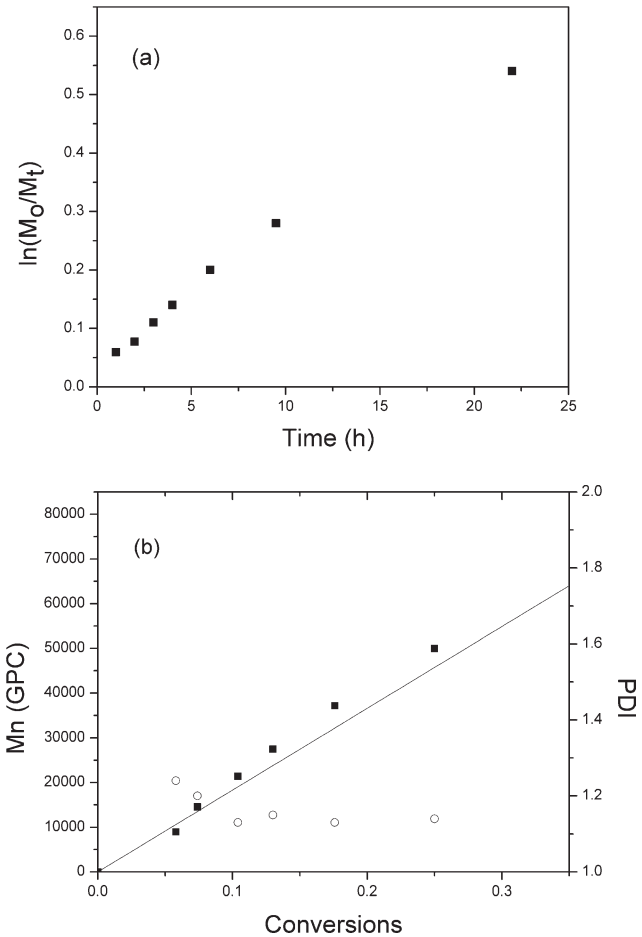

FIGURE 3 (a) Kinetic plots and (b) dependence of the GPC molecular weight (filled squares), theoretical molecular weight (solid line), and polydispersity (unfilled circles) on the conversion for the surface-initiated RAFT polymerization of *t*BuMA ([*t*BuMA]:[CPDB]:[AIBN] = 1000:1:0.1) with CPDB-anchored silica nanoparticles (RAFT surface density: 22.04 μmol/g) at 60 °C.

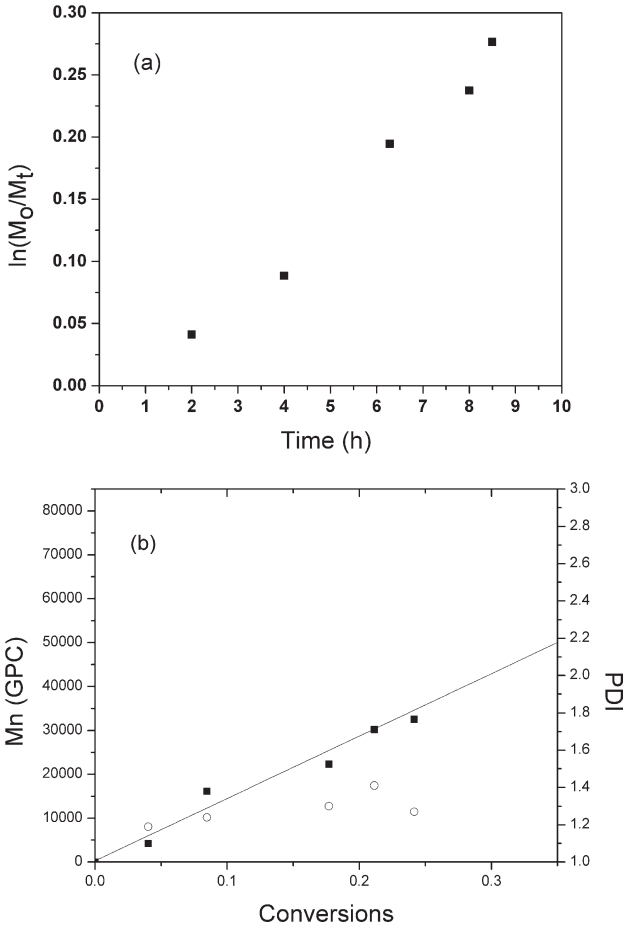

FIGURE 4 (a) Kinetic plots and (b) dependence of the GPC molecular weight (filled squares), theoretical molecular weight (solid line), and polydispersity (unfilled circles) on the conversion for the surface-initiated RAFT polymerization of *t*BuMA ([*t*BuMA]:[CPDB]:[AIBN] = 1000:1:0.1) with CPDB-anchored silica nanoparticles (RAFT surface density: 154.14 μmol/g) at 60 °C.

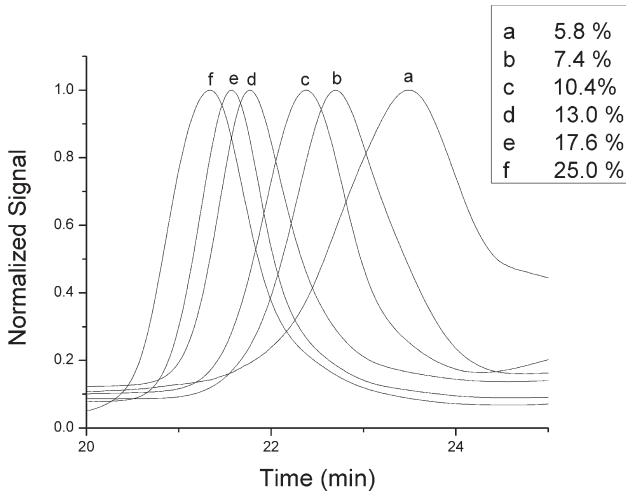

FIGURE 5 GPC traces for the RAFT polymerization of *t*BuMA mediated with surface-anchored CPDB at different conversions (a–f).

could not be easily redispersed. Deprotection of the *tert*-butyl ester proceeded in the presence of excess iodotrimethysilane; however, it was found that cleavage of the *tert*-butyl groups with TMSI in the presence of the thiocarbonylthio end groups yielded particles with ill-defined end groups and subsequently resulted in agglomeration. It was speculated that because of its Lewis acidic character, TMSI can coordinate to the thiocarbonyl end groups resulting in decomposition of the thiocarbonylthio to the free thiol followed by oxidative coupling that resulted in nanoparticle agglomeration. Therefore, poly(*t*BuMA) grafted nanoparticles were subjected to end group modification by treatment with excess AIBN prior to deprotection.[36,37] Conversion of the thiocarbonylthio end group proceeded smoothly and was confirmed by the disappearance of the strong absorption peak at 300 nm as indicated by UV–vis analysis in Figure 6. The newly modified particles were then exposed to excess TMSI to remove the *tert*-butyl groups as shown in Scheme 2.

Analysis of the nanoparticles by FTIR (Fig. 7) revealed the complete disappearance of strong absorption peaks representing the *tert*-butyl side chains at ~2900 cm^{-1} after treatment with TMSI. Furthermore, the appearance of a broad peak at 3500–2700 cm^{-1}, ascribed to the carboxylic—OH, and the broadening of the carbonyl stretch at 1700 cm^{-1} confirmed the successful formation of poly(MAA) grafted nanoparticles. The newly modified nanoparticles, decorated with thousands of acid moieties, displayed excellent solubility in alcoholic-based solvents, aqueous media, and mixtures thereof while remaining insoluble in solvents such as chloroform and THF. Figure 8 shows the ^{1}H NMR spectra of the polymer grafted silica nanoparticles before and after exposure to TMSI and further confirmed the successful formation of PAA grafted nanoparticles. The signal located at 1.40 ppm, arising from the *tert*-butyl groups completely disappeared

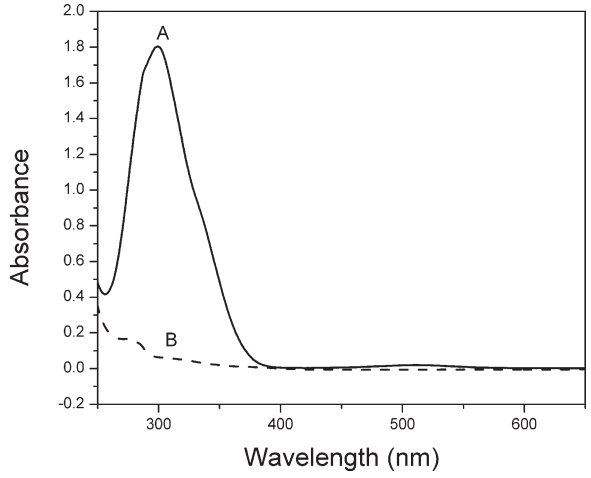

FIGURE 6 The UV-vis absorption spectra of poly(*t*BuMA) grafted silica nanoparticles (A) with thiocarbonylthio end group and (B) after treatment with AIBN.

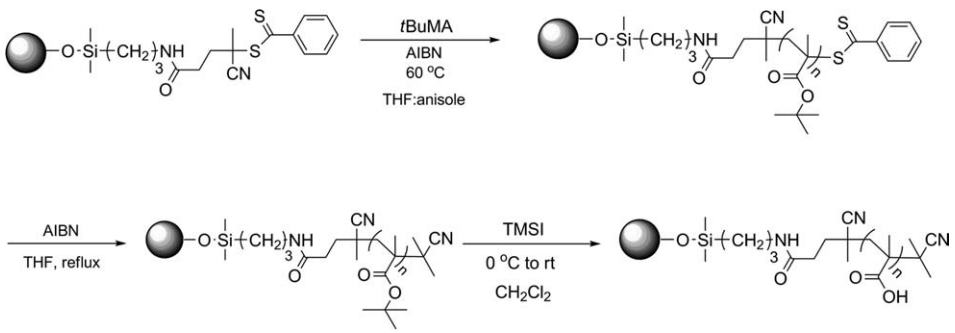

SCHEME 2 Synthesis of poly(*t*BuMA) particles, end group modification, and cleavage to poly(MAA).

following treatment with TMSI. Figure 9 shows the TGA in nitrogen of poly(MAA) grafted silica nanoparticles. The poly(MAA) (surface density: 0.23 chains/nm^2) accounted for 79.3% by weight in the nanocomposites, which was consistent with the UV analysis. Figure 10 shows the TEM image of poly(MAA) grafted silica nanoparticles and indicates that the diameter of the individual poly(MAA)-coated silica nanoparticles was around 30 nm.

EXPERIMENTAL

Materials

Unless otherwise specified, all chemicals were purchased from Acros and used as received. CPDB-anchored silica nanoparticles were prepared according to the literature.[26] *Tert*-butylmethacrylate (99%; Acros) was passed through basic alumina to remove inhibitor. AIBN was recrystallized from ethanol.

Instrumentation

NMR spectra were recorded on a Varian 300 using $CDCl_3$ or CD_3OD as the solvent. Molecular weights and molecular weight distributions were determined using a Waters gel permeation chromatograph equipped with a 515 HPLC pump, 2410 refractive index detector, three Styragel columns (HR1, HR3, and HR4 in the effective molecular weight range of 100–5000, 500–30,000, and 5000–500,000, respectively) with THF as eluent at 30 °C and a flow rate of 1.0 mL/min. The GPC system was calibrated with poly(methyl methacrylate) standards obtained from Polymer Labs. FTIR spectra were measured by a BioRad Excalibur FTS3000. UV–vis absorption spectra were taken on a Perkin-Elmer Lamda 4C UV–vis spectrophotometer.

Synthesis of Carboxylic Acid-Coated Nanoparticles Via Ring-Opening Reaction

Amine-functionalized silica nanoparticles were prepared according to the literature.[26] To a solution of amine-modified nanoparticles (330 mg, 41.7 μmol amine group) in THF (10 mL), succinic anhydride (42 mg, 0.417 mmol) was added as a 1 mM solution in DMF. The reaction was allowed to stir at room temperature (RT). After 16 h, the reaction solution was precipitated into diethyl ether (250 mL), and the particles were recovered by centrifugation at 5000 rpm for 10 min. The particles were dissolved in ethanol (5 mL) and reprecipitated in diethyl ether (150 mL). The particles were again collected by centrifugation and dispersed in ethanol (10 mL).

Preparation of Dye and Carboxylic Acid-Functionalized Silica Nanoparticles

NBD-NHS, N-[2-{N-(7′-Nitrobenz-2′-oxa-1′,3′-diazol-4′-yl)amino} ethyl-carbonyloxy] succinimide (2.72 mg, 7.786 μmol),

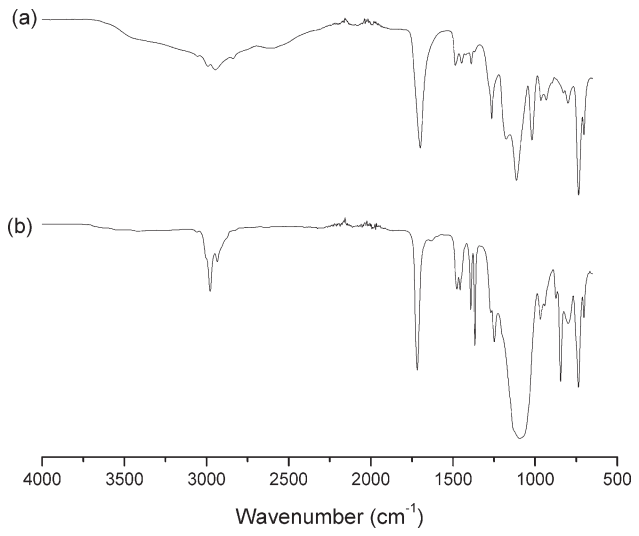

FIGURE 7 IR spectra of SiO_2-g-poly(*t*BuMA) (a) after and (b) before TMSI hydrolysis.

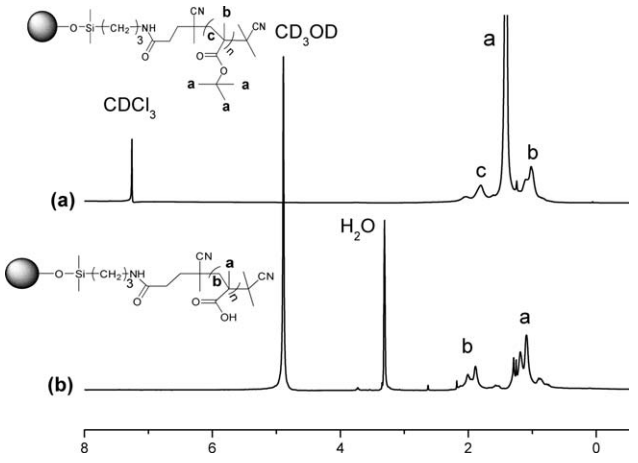

FIGURE 8 ^{1}H NMR spectra of nanoparticles grafted with (a) poly(*t*BuMA) and (b) poly(MAA) grafted silica nanoparticles.

as a solution in THF, was added dropwise to amino-functionalized silica nanoparticles (2.6 g, 56.9 μmol/g) dispersed in THF (30 mL). The reaction was stirred at RT. After 3 h, succinic anhydride (7.0 mg, 0.7 mmol) was added as a 1 mM solution in DMF, and the mixture was stirred overnight. The reaction solution was then poured into 200 mL of ethyl ether. The particles were recovered by centrifugation at 3000 rpm for 5 min. The particles were then redispersed in 30 mL of ethanol and reprecipitated in ethyl ether (200 mL). This procedure was repeated three more times until the supernatant remained colorless. The NBD-NHS and carboxylic acid-anchored silica nanoparticles were finally dissolved in ethanol (44.8 g/L). The NBD-NHS accounted for 4.8% in the total functionalized surface groups.

Graft Polymerization of *t*BuMA from CPDB-Anchored Silica Nanoparticles

In a dried Schlenk flask, CPDB-anchored silica (0.50 g, 22.04 μmol/g) was dissolved in THF (6.48 mL) followed by the addition of anisole (0.72 mL). To this solution, *t*BuMA (1.8 mL) and AIBN (220 μL, 0.005 M in THF) were added. The mixture was degassed by three freeze–pump–thaw cycles, back filled with nitrogen and then placed in an oil bath preset at 60 °C. A small of amount of the reaction mixture (1 mL) was withdrawn at various intervals to measure monomer conversion by NMR analysis. The polymerization was quenched by submersion of the reaction vessel in ice water. The polymer solution was precipitated into a methanol:water mixture (4:1), filtered, and dried under vacuum for 30 min. The polymer grafted particles were redispersed in THF, dried over magnesium sulfate, and filtered.

Cleavage of Grafted Poly(*t*BuMA) from Silica Nanoparticles

Typically, poly(*t*BuMA) grafted silica nanoparticles (20–30 mg) were dissolved in THF (3 mL). HF, hydrofluoric acid (0.5 mL, 49% in aq) was added to the solution and allowed to stir overnight at RT. The solution was poured into a PTFE Petri dish, and the volatiles were evaporated in a fume hood overnight. Following evaporation, the Petri dish was placed in vacuum oven for an additional 2 h. The recovered *t*BuMA polymer chains were dispersed in THF (1–2 mL) and subjected to GPC analysis.

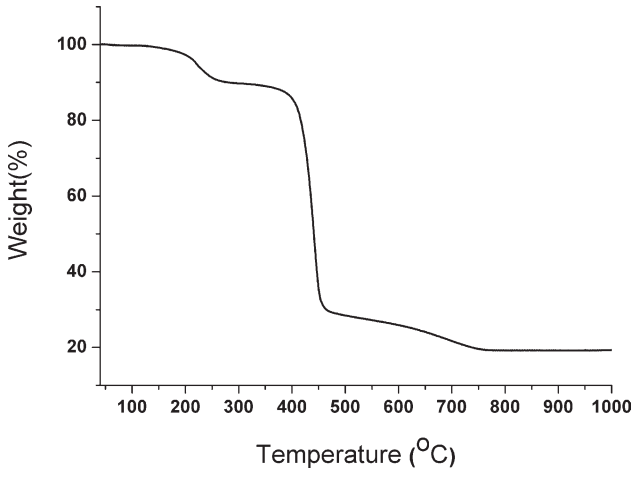

FIGURE 9 TGA in nitrogen of poly(MAA) grafted silica nanoparticles.

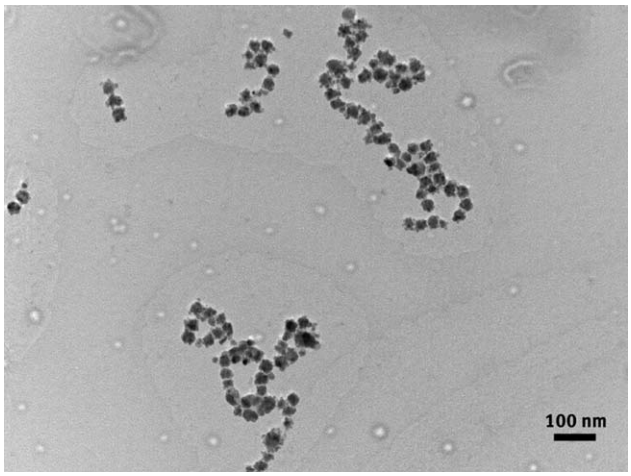

FIGURE 10 TEM image of poly(MAA) grafted silica nanoparticles.

Removal of Thiocarbonylthio End Group

A solution of poly(*t*BuMA) grafted silica nanoparticles (405 mg, 1 equiv end group) in THF (40 mL) was degassed with a stream of N_2 for 15 min followed by the addition of AIBN (40 mg, 10 equiv). The reaction was heated to reflux for 2 h and cooled to RT. The solution was concentrated to ~10 mL *in vacuo* and precipitated into a methanol:water mixture (4:1). The polymer solution was filtered and dried under vacuum for 30 min. The polymer grafted particles were redispersed in CH_2Cl_2, dried over sodium sulfate, and filtered.

Ester Cleavage of Poly(*t*BuMA)

A solution of poly(*t*BuMA) grafted silica nanoparticles (400 mg, 1 equiv of *tert*-butyl) in CH_2Cl_2 (50 mL) was cooled to 0 °C. TMSI (4 mL, 10 equiv) was added dropwise to the solution. The solution was allowed to warm to RT and stirred for an additional 16 h. The solution was concentrated under reduced pressure and precipitated into diethyl ether. The polymer was redispersed into methanol. This dissolution–precipitation process was repeated until the polymer remained white.

CONCLUSIONS

A convenient method for the preparation of silica nanoparticles bearing carboxylic acid residues was developed. First, a monolayer of carboxylic acid residues was attached to the nanoparticles by treating amino-modified particles with succinic anhydride. Furthermore, the addition of a small amount of an amine reactive fluorescent dye followed by excess succinic anhydride yielded bifunctional nanoparticles. Second, surface-initiated RAFT polymerization of *t*BuMA from the surface of the silica nanoparticles was conducted to yield grafted polymers with controlled molecular weights and narrow polydispersities. Postmodifications of the surface grafted polymer were successfully performed to convert the

thiocarbonylthio into a stable end group followed by removal of the *tert*-butyl ester to yield poly(MAA) grafted silica nanoparticles. The synthesis of the poly(MAA) brushes was confirmed with FTIR and ^{1}H NMR analysis. These procedures provide a simple and useful way to prepare carboxylic acid-functionalized nanoparticles with a wide range of surface attached acid densities, which can be easily redispersed in common solvents.

ACKNOWLEDGMENTS

The authors gratefully acknowledge the NSF (BME-1032579) for supporting this work.

REFERENCES AND NOTES

1 Chiefari, J.; Chong, Y. K.; Ercole, F.; Krstina, J.; Jeffery, J.; Le, T. P. T.; Mayadunne, R. T. A.; Meijs, G. F.; Moad, C. L.; Moad, G.; Rizzardo, E.; Thang, S. H. *Macromolecules* **1998,** *31*, 5559–5562.

2 Handbook of RAFT Polymerization; Barner-Kowollik, C., Ed.; Wiley-VCH: Weinheim, Germany, **2008.**

3 Lowe, A. B.; McCormick, C. L. *Aust. J. Chem.* **2002,** *55*, 367–379.

4 Moad, G.; Rizzardo, E.; Thang, S. H. *Aust. J. Chem.* **2005,** *58*, 379–410.

5 Moad, G.; Rizzardo, E.; Thang, S. H. *Aust. J. Chem.* **2006,** *59*, 669–692.

6 Gangopadhyay, R.; De, A. *Chem. Mater.* **2000,** *12*, 608–622.

7 Sun, Y. P.; Riggs, J. E. *Int. Rev. Phys. Chem.* **1999,** *18*, 43–90.

8 Sanchez, C.; Lebeau, B.; Chaput, F.; Boilot, J. P. *Adv. Mater.* **2003,** *15*, 1969–1994.

9 Ohno, K.; Ma, Y.; Huang, Y.; Mori, C.; Yahata, Y.; Tsujii, Y.; Maschmeyer, T.; Moraes, J.; Perrier, S. *Macromolecules* **2011,** *44*, 8944–8953.

10 Tsujii, Y.; Ejaz, M.; Sato, K.; Goto, A.; Fukuda, T. *Macromolecules* **2001,** *34*, 8872–8878.

11 Barbey, R.; Lavanant, L.; Paripovic, D.; Schúwer, N.; Sugnaux, C.; Tugulu, S.; Klok, H. A. *Chem. Rev.* **2009,** *109*, 5437–5527.

12 Li, Y.; Schadler, L.; Benicewicz, B. In Handbook of RAFT Polymerization; Barner-Kowollik, C., Ed.; Wiley-VCH: Weinheim, Germany, **2008;** Chapter 11, pp 423–453.

13 Treat, N. D.; Ayres, N.; Boyes, S. G.; Brittain, W. J. *Macromolecules* **2006,** *39*, 26–29.

14 Stuart, M. A. C.; Huck, W. T. S.; Genzer, J.; Müller, M.; Ober, C.; Stamm, M.; Sukhorukov, G. B.; Szleifer, I.; Tsukruk, V. V.; Urban, M.; Winnik, F.; Zauscher, S.; Luzinov, I.; Minko, S. *Nat. Mater.* **2010,** *9*, 101–133, and references therein.

15 Wu, T.; Gong, P.; Szleifer, I.; Vlcek, P.; Šubr, V.; Genzer, J. *Macromolecules* **2007,** *40*, 8756–8764.

16 Li, D.; Sheng, X.; Zhao, B. *J. Am. Chem. Soc.* **2005,** *127*, 6248–6256.

17 Hojjati, B.; Sui, R.; Charpentier, P. A. *Polymer* **2007,** *48*, 5850–5858.

18 Inoue, M.; Fujii, S.; Nakamura, Y.; Iwasaki, Y.; Yusa, S. *Polym. J.* **2011,** *43*, 778–784.

19 Klevens, R. M.; Edwards, J. R.; Richards, C. L.; Horan, T. C.; Gaynes, R. P.; Pollock, D. A.; Cardo, D. M. *Public Health Rep.* **2002,** *122*, 160–165.

20 Drenkard, E.; Ausubel, F. M. *Nature* **2002,** *416*, 740–743.

21 Fuqua, W. C.; Parsek, M. R.; Greenberg, E. P. *Annu. Rev. Genet.* **2003,** *35*, 439–468.

22 Miller, M. B.; Bassler, B. L. *Annu. Rev. Microbiol.* **2001,** *55*, 165–199.

23 Fuqua, W. C.; Greenberg, E. P. *Nat. Rev. Mol. Cell Biol.* **2002,** *3*, 685–695.

24 Tom, R. T.; Suryanarayanan, V.; Reddy, P. G.; Baskaran, S.; Pradeep, T. *Langmuir* **2004,** 1909–1914.

25 Turos, E.; Shim, J. Y.; Wang, Y.; Greenhalgh, K.; Reddy, G. S. K.; Dickey, S.; Lim, D. V. *Bioorg. Med. Chem. Lett.* **2007,** *17*, 53–56.

26 Li, C.; Han, J.; Ryu, C. Y.; Benicewicz, B. C. *Macromolecules* **2006,** *39*, 3175–3183.

27 An, Y.; Chen, M.; Xue, Q.; Liu, W. *J. Colloid. Interface Sci.* **2007,** *311*, 507–513.

28 Li, C.; Benicewicz, B. C. *Macromolecules* **2005,** *38*, 5929–5936.

29 Mayer, T. G.; Weingart, R.; Münstermann, F.; Toshinari, K.; Kurzchalia, T.; Schmidt, R. R. *Eur. J. Org. Chem.* **1999,** *10,* 2563–2571.

30 Chong, Y. K.; Le, T. P. T.; Moad, G.; Rizzardo, E.; Thang, S. H. *Macromolecules* **1999,** *32*, 2071–2074.

31 Yang, C.; Cheng, Y. L. *J. Polym. Sci. Part A: Polym. Chem.* **2006,** *102*, 1191–1201.

32 Hosseini Nejad, E.; Castignolles, P.; Gilbert, R. G.; Guillaneuf, Y. *J. Polym. Sci. Part A: Polym. Chem.* **2008,** *46*, 2277–2289.

33 Pelet, J. M.; Putnam, D. *Macromolecules* **2009,** *42*, 1494–1499.

34 Chaduc, I.; Lansalot, M.; D'Agosto, F.; Charleux, B. *Macromolecules* **2012***, 45,* 1241–1247.

35 Cowie, J.; Arrighi, V. Polymers: Chemistry and Physics of Modern Materials, 3rd ed.; CRC: FL, USA, **2007;** Chapter 3, p 65.

36 Chen, M.; Moad, G.; Rizzardo, E. *J. Polym. Sci. Part A: Polym. Chem.* **2009,** *47*, 6704–6714.

37 Perrier, S.; Takolpuckdee, P.; Mars, C. *Macromolecules* **2005,** *38*, 2033–2036.